

Optimisation of construction of two-channel acousto-optic modulator for radio-signal phase detection

L. JODŁOWSKI*

Institute of Optoelectronics, Military University of Technology
2 Kaliskiego Str., 00-908 Warsaw, Poland

Two-channel acousto-optic modulator (AOM) makes simultaneous assignment of the frequency and phase of radio-signals possible. AOM is a fundamental element of a spectrum analyser based on acousto-optic receiver. In the paper, an analysis of influence of structural elements on characteristics of a two-channel modulator was shown and the procedure of optimisation of its construction described. Basing on this procedure the modulator for spectrum analysis at GSM band was designed, performed and investigated. The two-channel acousto-optic modulators give the possibility of detection and defining direction of radiation with accuracy of 0.5° .

Keywords: acousto-optics, modulator, phase detection.

1. Introduction

Acousto-optic modulators (AOM) are based on elasto-optic effect which allows transfer of information from acoustic wave to light beam. AOM are commonly applied in RF signal analysers. The possibility of performing Fourier analysis of high frequency radio signal in real time is their major advantage. Practical implementation of AOM is possible since high sensitivity CCD linear arrays have been built. Elaboration of CCD cameras enabled one to carry out two-dimensional analysis of an image in a focus of analysing system. Thus, simultaneous analysis of frequency and phase of radio signal became possible.

Two-channel acousto-optic modulator is an upgraded version of acousto-optic deflector and was not described in available literature [1,2]. Acousto-optic deflectors are used in signal analysers [3,4] and broadband and fast signal analyses [5] are their major advantages. Spectral analysis is carried out in real time without any time delay. Acousto-optic modulator designed for measuring radio signal phase contains, compared to deflector, a second channel (reference one) and signal is analysed in XY image plane. Like for deflector, optimisation of construction consists in elaboration of main structural elements:

- active material and its orientation,
- optical aperture of modulator,
- material and orientation of piezoelectric transducer,
- central frequency and bandwidth of transducer,
- configuration and size of electrodes,
- matching circuits.

* e-mail: jodle@wat.edu.pl

The problem of cross-talk signals is difficult to predict and is presented elsewhere [6]. Analysis of properties of the two-channel modulator for structural optimisation is the main goal of the paper.

2. Analysis of influence of structural elements on characteristics of two-channel modulator (deflector)

2.1. Characteristics of the modulator

An arrangement scheme for analysis of radio-signal phase is shown in Fig. 1. Separated blocks represent: light source (laser), beam forming optics, two-channel acousto-optic modulator, analysing optics and elements of image registration and analysis (CCD camera, PC computer with frame-grabber card). Collimating optics is used to obtain uniform intensity distribution of laser beam in the area of acousto-optic modulator's part overtaken by acoustic beam. As a result of acousto-optic effect part of laser beam is deflected with an angle proportional to frequency of electric signal. Analysing optics (lens) separates and focuses deflected and main beams in different places, so in an image plane of CCD camera only deflected beam is visible.

A structural scheme of the two-channel acousto-optic modulator is presented in Fig. 2(a). Interaction between light beam and ultrasonic wave takes place in an acoustic buffer region (1). Ultrasonic beam is generated and formed by the piezoelectric transducer (2) with the electrodes (5) of dimensions $d \times l$. The length of ultra-

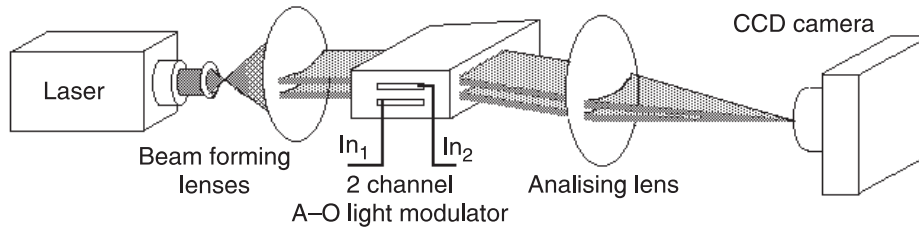


Fig. 1. Scheme of a system for analysis of radio-signal phase with use of two-channel A-O modulator. In₁ and In₂ are the signal and reference inputs, respectively.

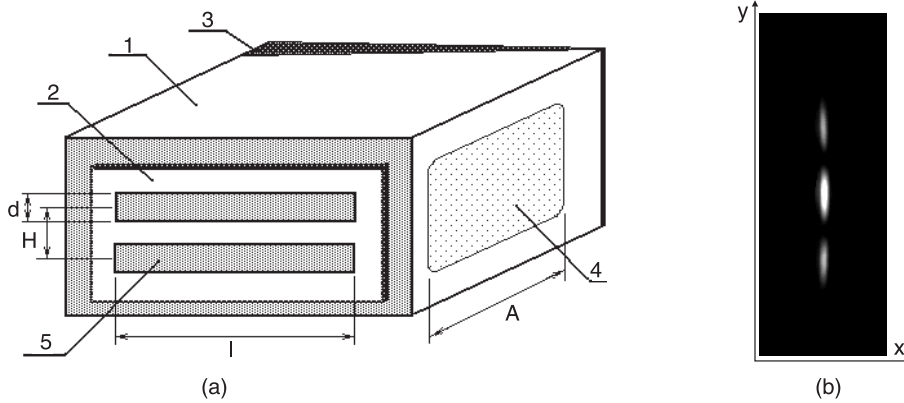


Fig. 2. Details of construction of A-O modulator (a) and a CCD picture (b) taken in a laboratory setup.

sound-light interaction equals A (the width of optical window (4)). A distance between parallel electrodes is H . The absorber (3) is intended for attenuation of acoustic wave after having passed the whole buffer. An interference picture recorded by CCD camera is shown in Fig. 2(b). Projection of interference picture on x axis gives information about frequency of signal utilised in a spectrum analyser. Distribution of light intensity at y direction depends on differences between phases of analysed and reference signals.

2.2. Buffer material, conversion efficiency, and attenuation of acoustic wave

Bragg diffraction is used to describe phenomena in acousto-optic deflectors [5]. A diffraction mode depends on light and sound wave frequencies as well as on length of interaction. The Cook parameter is a criterion for estimating a diffraction mode [1]

$$Q = \frac{\lambda_0 l F_0^2}{n V^2}, \tag{1}$$

where λ_0 is the wavelength of light beam, l is the length of ultrasound interaction (length of transducer), n is the index of refraction, F_0 and V are the frequency and the velocity of ultrasound wave, respectively.

So, for $Q < 1$ Raman-Nath mode of diffraction occurs and for $Q > 1$ Bragg diffraction takes place. Bragg diffrac-

tion occurs when angles of incidence of both light and acoustic beams fulfil Bragg condition

$$\sin \Theta_B = \frac{\lambda_0}{2L}, \tag{2}$$

where L is the wavelength of acoustic wave, and Θ_B is the Bragg angle.

Deflected beams appear in +1 or -1 diffraction orders and they change their frequencies according to the following dependence

$$\omega_1 = \Omega + \omega_0 \quad (\text{for } +1 \text{ order}).$$

In linear regime (up to 60–70% of modulation) diffraction efficiency depends on energy of acoustic wave and acousto-optical quality factor

$$a_0 = \frac{54\eta}{P_e M_2} \frac{d}{l} \left(\frac{\lambda}{\lambda_1} \right)^2, \tag{3}$$

where l and d are the length and the width of transducer, respectively, M_2 is the relative quality factor of buffer (compared with quality factor for fused quartz), λ and λ_1 are the wavelengths of applied and He-Ne lasers, respectively, η is the diffraction efficiency and α_0 is the efficiency of electric energy conversion into acoustic wave energy.

In Table 1, data of materials chosen for acousto-optic media are presented. The most important parameters are

Table 1. Characteristics of acousto-optic materials suitable for longitudinal wave propagation.

Material	$\rho \times 10^3$ (kg/m ³)	$V \times 10^3$ (m/s)	$M_2 \times 10^{15}$ (c ³ /kg)	α (dB/GHzcm)	λ_0 (μ m)	T Transparency (μ m)	n
Fused quartz	2.20	5.96	1.56	12	0.63	0.2–4.5	1.457
GaP	4.13	6.32	44.6	6	0.63	0.6–10	3.31
PbMoO ₄	6.95	3.63	36.3	15	0.63	0.42–5.5	0.42–5
TeO ₂	5.87	3.40	34.5	10	0.63	0.35–5	2.26
Ge	5.38	5.5	260	30	10.6	2.0–20	4
Te	5.25	2.29	5860	420	10.6	4.0–20	2.29
LiNbO ₃	4.63	6.57	7	0.15	0.63	0.4–4.5	2.29
SF4 ¹ (CF 755-28)	4.79	3.76	7.2	110	0.63	0.4–4	1.75
SF8 ¹ (CF 689-31)	4.21	3.89	6.3	50	0.63	0.4–4	1.685
SF14 ¹ (CF 762-27)	4.5	4.059	5.6	35	0.63	0.4–4	1.756
BK 7	2.53	5.53			0.63	0.34–4	1.517

¹ measurements of attenuation [13] were made for 50–250 MHz band

the following: the quality factor M_2 , the attenuation of acoustic wave α , and the range of optical transparency T . For isotropic materials diffraction efficiency depends on incidence angle of light beam and is the largest for Bragg angle, so this condition occurs for one frequency only. For higher and lower frequencies decrease in diffraction efficiency is observed and this can be compensated using external matching circuit (matching filter) [7].

Attenuation of acoustic wave in material decreases its intensity with a increasing distance from transducer surface and causes decrease in diffraction efficiency via limitation of effective aperture. This phenomenon is strictly connected with deflector resolving power. As it was shown in Ref. 1, a 25 dB attenuation at aperture region causes 30% worsening of resolving power.

For acoustic powers less than optimal ones diffraction efficiency meets twofold decrease if attenuation equals 8 dB at aperture region. Increasing acoustic power can improve it. So, after having attenuation compensated, a serious 40–50% improvement in diffraction efficiency can be obtained for 10–20 dB attenuation at aperture region. As a result, intensity of light decreases not more than 40–50%.

Piezoelectric crystals are commonly used for transducers converting electrical energy to mechanical one. Numerous investigations showed [8,9] that transducers based on LiNbO₃ crystals or on deposited TeO₂ layers are the best for longitudinal wave generation.

2.3. Resolving power of deflector

Scanning angle of the deflector $\Delta\theta_d$ depends on acoustic frequency band and is described as follows

$$\Delta\theta_d = \left(\frac{p\lambda}{nV} \right) \Delta F, \quad (4)$$

where λ is the length of optic wave, p is the number of diffracted order, ΔF is the frequency band of acoustic wave, n is the refractive index, and V is the acoustic wave speed.

The number N of resolved positions of deflected beam depends on angular width φ_d of a light beam

$$N = \frac{\Delta\theta_d}{\varphi_d}. \quad (5)$$

If φ_d angle depends only on diffracted effect connected with a finite size of light beam, then

$$\varphi_d = \frac{\mu\lambda}{nA} \quad (6)$$

where μ is the parameter depending on a light beam structure and a criterion of resolving power, A is the size of the light beam (aperture).

For instance, according to Rayleigh's criterion the two beams are considered as resolved if maximum of the first beam overlaps with a minimum of the second one. Then the parameter μ equals 1 for homogeneous rectangular beam, while μ equals 1.22 for homogeneous circular beam and μ equals 1.34 for Gaussian beam.

This criterion is very strict, so other criteria of resolution are also used. For rectangular light beam of homogeneous intensity distribution ($\mu = 1$) we have

$$N = \frac{\Delta FA}{V} = \Delta F \tau \quad (7)$$

where τ is the time-of-flight of acoustic wave passing aperture of deflector (τ additionally defines switching rate).

Equation (7) relates two fundamental characteristics of deflector: resolution and switching rate. Analysis of solution of the equation shows two ways for resolution improvement: increase in acoustic band or increase in light beam size. However, the second way simultaneously decreases switching rate.

2.4. Interference of the deflected beams in a focus

If the lens aperture and focus are D and f , respectively, (see Fig. 3(a)), the light intensity distribution in a focus can be described as follows

$$I(y) = [\text{sinc}(x)]^2, \tag{8}$$

where function $\text{sinc}(x)$ is the standard function: $\text{sinc}(x) = \sin x/x$.

The first minimum of intensity distribution occurs for the angle β as

$$\beta = \frac{1.22\lambda}{A}. \tag{9}$$

For small angles, β can be expressed as $\beta = x/f$; so the function sinc has its first zero value for the argument $Py = \pi$. If so, then

$$P = \frac{\pi d}{\mu\lambda f}, \tag{10}$$

where d is the height of transducer, μ is the parameter of distribution (described in previous section), λ is the wavelength of light beam, and f is the lens focus. Both light beams carrying information about acoustic signal phase interfere in a focus.

The distance between interference maxima depends on heights H of beams and focal length of the analysing lens [see Fig. 3(b)]. So, the function sinc is “modulated” by the harmonic function (eg., \cos) with an argument

$$\left(2\pi \frac{H}{\lambda f} y + \varphi\right), \tag{11}$$

where H is the distance between the transducers and φ is the phase of acoustic signal.

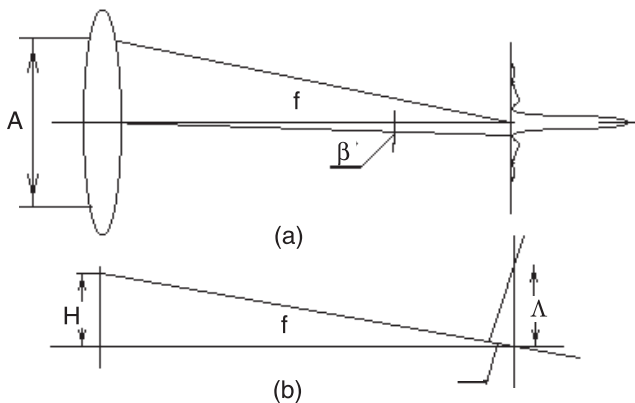


Fig. 3. Light intensity distribution in a focus (a) and interference pattern (b) from sources positioned at a distance H .

Final formula for distribution of light intensity in a focus of analysing lens is the following

$$I(y) = \left(\frac{\sin\left(\frac{\pi d}{\mu\lambda f} y\right)}{\frac{\pi d}{\mu\lambda f} y} \right)^2 \left[1 + \cos\left(2\pi \frac{H}{\lambda f} y + \varphi\right) \right], \tag{12}$$

where d is the height of transducer, μ is the parameter of distribution (described in previous section), λ is the wavelength of light beam, f is the lens focus, H is the distance between transducers, and φ is the phase of the acoustic signal.

2.5. Central frequency and transducer bandwidth

From generator side, piezoelectric transducer has complex impedance [10]. Electric matching between transmitter (generator) and receiver (transducer) is necessary to ensure optimal propagation of electric energy. Since input impedance of the transducer is a complex function of structural parameters (including also acoustic and mechanical properties of layers connecting piezoelectric transducer and a buffer) the analysis of the system is not simple [11,12]. In general, surface of the transducer and a difference in acoustic impedances between the transducer and the buffer have major influence on band narrowing. Even using matching Γ type circuits, different electric bandwidths can be obtained for the same transducer. Details are presented in Ref. 12.

An equivalent circuit described by Mason [10] was applied to carry out an analysis of transducer’s electric impedance. Figure 4(a) shows a scheme of transducer for analysis of electric impedance. Transducer plate of thickness d and of acoustic impedance Z_0 is placed between the waveguide and absorber of impedances Z_b and Z_a , respectively. The voltage e_3 is connected to terminals 3–3 and the current i_3 is flowing through the transducer. Equivalent scheme of the transducer is shown in Fig. 4(b). According to equivalent scheme quantities characterising the transducer and adjacent media are transformed into the electric impedance.

For one-sided load (buffer loaded by Z_l impedance), input impedance can be described as follows

$$Z = R_3 + j\left(X_3 - \frac{1}{\omega C_0}\right), \tag{13}$$

where

$$R_3 = R_a \left(\frac{f_0}{f_r}\right)^2 H_r, \tag{14}$$

$$X_3 = R_a \left(\frac{f_0}{f_r}\right)^2 H_i, \tag{15}$$

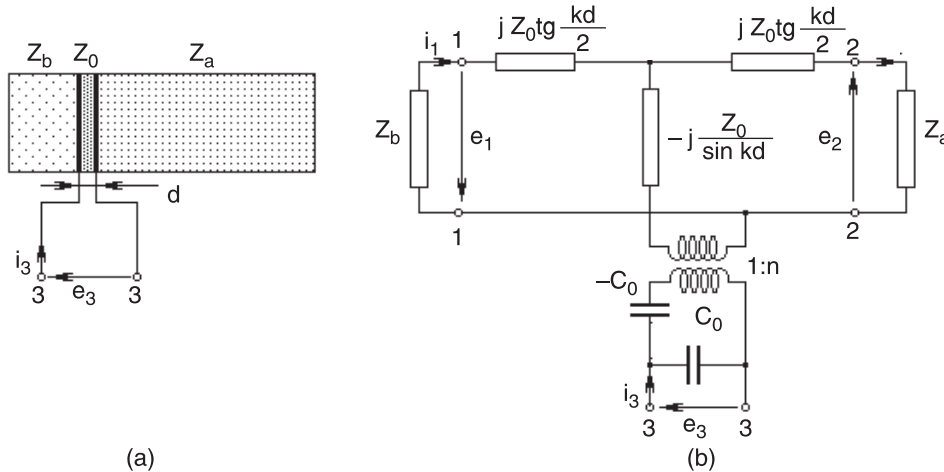


Fig. 4. Piezoelectric transducer. Transducer scheme (a) and equivalent scheme (b).

$$R_a = \frac{\pi Z_0}{4 Z_l} \frac{k_0^2}{\omega_0 C_0}, \quad (16)$$

$$r = \frac{R_g}{|Z|}, \quad (19)$$

$$H_r = \frac{1}{4} \left(\frac{Z_l}{Z_0} \right)^2 \frac{[1 - \cos(kd)]^2}{[\sin(kd)]^2 + \left(\frac{Z_l}{Z_0} \cos(kd) \right)^2}, \quad (17)$$

where R_g is the resistance of generator (usually 50Ω) and Z is the load impedance.

Standing wave ratio (SWR) is defined as follows

$$SWR = \frac{1 + |\Gamma|}{1 - |\Gamma|}, \quad (20)$$

where $|\Gamma| = (1 - r)/(1 + r)$.

Expressing load impedance in a normalised form as $Z = R + jX$, the quantity Γ can be expressed by real and imaginary parts of the impedance

$$|\Gamma| = \frac{\sqrt{(R^2 - 1 + X^2)^2 + 4X^2}}{(R + 1)^2 + X^2} \quad (21)$$

$$H_i = \frac{1}{2} \frac{Z_l}{Z_0} \frac{\sin(kd) \left(1 + \left(\frac{1}{2} \left(\frac{Z_l}{Z_0} \right)^2 - 1 \right) \cos(kd) \right)}{[\sin(kd)]^2 + \left(\frac{Z_l}{Z_0} \cos(kd) \right)^2}, \quad (18)$$

and $kd = \pi \frac{f}{f_0}, \quad f_0 = \frac{V}{2d}, \quad C_0 = \epsilon_0 \epsilon_w \frac{S}{d}.$

In Eqs. 13–18, influence of the connecting layers on electric impedance of the transducer was neglected. The influence of connecting layers can be neglected up to the frequencies 100–150 MHz for metallic layers of 1- μm thickness. For higher frequencies an influence of the layers must be taken into consideration [11].

2.6. Electrical matching between transducer and measuring circuit

Parallel or series inductive coil can be used as a matching circuit for some cases. Although transducer operation without matching circuit is possible such solution is used for acoustic measuring heads rather than for acousto-optic modulators [12]. Since full impedance matching for the transducer occurs for chosen frequencies only, a suitable criterion for evaluation of matching is based on, so called, standing wave ratio (SWR). This parameter is measured in a typical operational mode of network analysers. Reflection coefficient r of incident wave depends on load impedance

A criterion for sufficient matching for the transducer is $SWR < 1.5$. When receiver impedance and circuit impedance are fully matched SWR equals 1, while for short and open circuits it reaches infinity. For example, for 3dB electric band attenuation SWR amounts 6.

On the other hand, insufficient impedance matching leads to reflection of electric power at impedance drop and as a result significantly lower electric power is delivered to the circuit. Moreover, time of oscillations fading increases and a deformation of pulse shape is observed. It is particularly undesirable for short pulses when the period of oscillations fading and pulse duration at impedance discontinuity are comparable

$$t_i \leq \frac{g}{V}, \quad (22)$$

where g is the thickness of transducer and V is the speed of sound in transducer.

A frequency shift for maximum radiation towards lower frequencies is another effect observed for loaded transducer, so the optimal thickness of transducer g is smaller than that calculated for free oscillations ($\lambda/2$)

$$g \leq \frac{V}{2F_0}. \quad (23)$$

Example: for 20 MHz frequency pulse deformation is observed for 25 ns pulses, while for higher frequencies deformation occurs for shorter pulses.

In many cases the single-element Γ filters can be used as matching circuits. A bandwidth of matched transducer depends on its impedance and filter configuration. More detailed analysis showed that larger bandwidth of electrical matching can be obtained when real part of transducer impedance is close to impedance of generator (transmitting line) [12]. In calculations, both parallel and series equivalent circuits must be taken into account. Generally, four basic configurations of Γ type matching circuits must be analysed to make a proper choice of optimal configuration [11].

The use of multi-element filters is a brand new quality in matching technique. Theory of calculation of these circuits is well known but it has not been used in transducers matching for years [14]. The calculations of filters were as sophisticated and difficult, as their manufacturing and measurements were complex. An improvement in computing and measuring techniques allows for application of multi-element matching circuits in optimisation of piezoelectric transducers. For acousto-optic devices this method compensates angular dependence of diffraction efficiency and acousto-optic characteristics are more flat [7].

Basing on structural and material data of elements used (transducer, connecting layers, buffer, electrodes and load), one can calculate electrical characteristics of transducer (electric impedance) and next, optimal single- or multi-element matching circuits of Γ type and theoretical characteristics of electrical impedance of transducer. This task is presented in the next section.

3. Procedure for calculating optimal construction of the modulator

The procedure is performed through a few steps in which the following parameters are defined: aperture of detector, central frequency of deflector, transducer length and high, electric power, and distance between electrodes.

3.1. Aperture of deflector

Aperture (A) of the deflector is limited by attenuation of acoustic wave in buffer, so

$$A \leq \frac{\alpha_d}{\alpha_0 F_0^2}, \quad (24)$$

where α_d is the acceptable attenuation in aperture region (ordinary 3 dB), α_0 is the coefficient of attenuation of acoustic wave, and F_0 is the approximated central frequency of transducer.

Aperture calculated here is of rather theoretical meaning, since deflector can operate with attenuation even up to 20 dB. This was discussed in a more detailed way in Section 2.2.

3.2. Central frequency of deflector

Central frequency can be calculated assuming larger bandwidth (60%). Since deflectors operate at transitive mode of diffraction, acoustic beam has some angular divergence and the largest bandwidth of interaction occurs for Cook's parameter $Q = 3.7$ (see Section 2.2) and equals $0.6 f_0$ [1]. This frequency band can be obtained using LiNbO₃ piezoelectric transducers. Transforming Eq. (7) we have

$$F_0 = \frac{NV}{0.6A}, \quad (25)$$

where N is the number of resolved points (determining resolving power of the deflector), V is the speed of acoustic wave, and A is the size of light beam (aperture) calculated in previous step.

Three parameters which describe deflector are coupled: resolution (N), switching rate or aperture (τ, A) and a bandwidth (central frequency f_0 and parameter Q). So, the procedure of defining central frequency and aperture (steps 1 and 2) must be repeated until they satisfactorily fulfil the requirements.

3.3. Length of transducer

The optimal length (l) of the transducer can be calculated from the defined parameter Q ($Q = 3.7$)

$$l = 3.7 \frac{nV^2}{\lambda F_0^2} \quad (26)$$

where λ is the wavelength of light beam, n is the index of refraction, F_0, V are the frequency and the velocity of ultrasound wave.

3.4. Height of transducer

Height of the transducer (d) can be calculated from the condition of divergence of acoustic beam. The height of transducer must assure that the whole aperture should be located within near field of the transducer

$$d = \sqrt{A \frac{V}{F_0}}, \quad (27)$$

where the symbols are the same as in Section 3.3.

3.5. Required electric power

Electric power depends on efficiency of energy conversion from electric energy into acoustic one (α) and on depth of diffraction (η). The following formula describes electric power

$$P_A = \alpha P_E = \frac{54\eta}{M_2} \frac{d}{l} \left(\frac{\lambda}{\lambda_0} \right)^2, \quad (28)$$

where α is the efficiency of energy conversion, P_E is the delivered electric power, l, d are the length and the width of transducer, respectively, M_2 is the relative acousto-optical quality factor of medium (compared to fused quartz), η is the diffraction depth, λ, λ_1 are the wavelengths of applied light beam and reference laser (He-Ne), respectively.

3.6. Distance between electrodes H

Intensity distribution of light resulting from phase difference of electric signals in the two paths should assure the best measurement conditions. This means that in an interference pattern two interference maxima must be apparent. As a result of theoretical analysis (Eq. 12 and Ref. 15) this condition is fulfilled when

$$H = 2.25d, \quad (29)$$

where d is the width of the transducer.

Generally, all these optimisation calculations are difficult, however can be solved with use of our software.

4. Exemplary calculations of two-channel deflector

Results of calculations are presented in Table 2. The calculations of electric matching were carried out for the transducer attached to a buffer with metallic Cr-Au-In layer [16]. Optimum radiation of the transducer was calculated for 220 MHz (central frequency) while maximum of real part of impedance was found for intermediate frequency of 140 MHz.

Matching was performed with simple single-element circuits of Γ type. For matching with circuit *a* [Fig. 5(a)] it gave a 3 dB electric band in the range of 124–157 MHz, while for circuit *b* [Fig. 5(b)] matching occurred at 117–181 MHz. Although the latter gave larger bandwidth yet a proper operation of the transducer was not achieved. Only the use of two-branch LC circuit shown in Fig. 5(c) resulted in a symmetric electric band larger than necessary for properly optimised deflector. In table c, attached to Fig. 5(c), the values of LC elements of the filter are shown. It was the optimal configuration.

5. Experimental verification

Investigations of modulators were carried on laboratory stand described in Ref. 17. A PC controlled generator could precisely change phase of electric signal delivered to the modulator. The system of recording interference pattern enabled both on-line operation as well as operation on data stored earlier in the system memory.

Construction data and experimental errors of phase measurements are shown in Table 3 for preliminary model (described as a model 0) and for models optimised according to the procedure presented in the paper. The modulators were

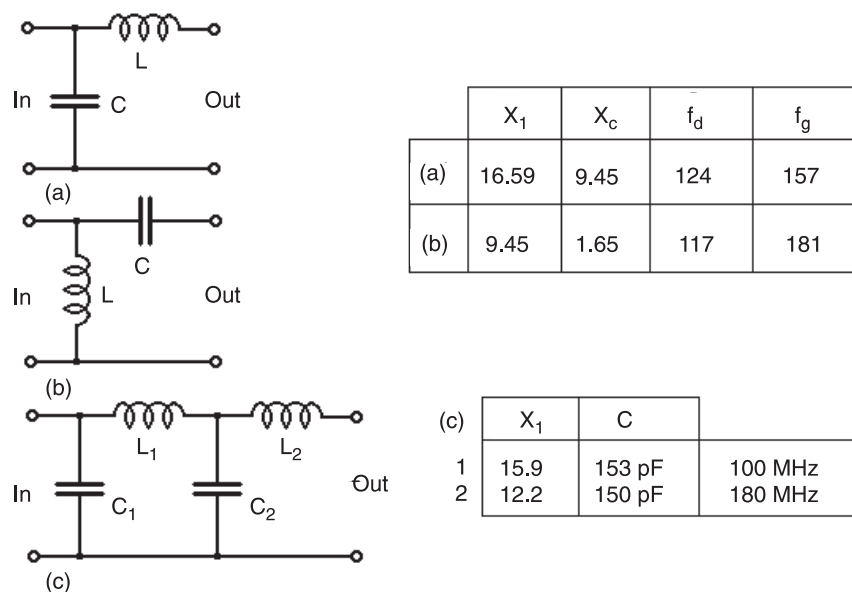


Fig. 5. Comparison of transducers matching with use of: single element Γ type filters (a and b), and two-element filter (c). For the filter c full matching occurs at band borders (100 and 180 MHz, respectively). Matching with a and b filters is not satisfactory, the use of four-element filter is much better.

Table 2. Results of calculations for the two-channel deflector based on SF 4 glass.

Calculation of aperture			Units used	Values	SI units
Acceptable attenuation in aperture region			dB	5	
Attenuation coefficient			dB/GHz×cm	110	
Central frequency			GHz	0.14	
Calculated admissible aperture	cm	2.32			
Calculation of F_0					
Aperture			cm	2.1	0.01
Velocity of acoustic wave			km/s	3.89	1.00E+03
N (number of points)				500	
Calculated F_0	MHz	139.26			
Optimised length of transducer					
Accepted frequency			MHz:	140	1.00E+06
Refraction index			n	1.685	
Wavelength of light beam			μm	0.63	1.00E-06
Maximum bandwidth (60% for $Q = 3.7$)	MHz:	84			
Calculated length of transducer	mm:	6.78			
Accepted length of transducer			mm	6.8	
Acceptable height of transducer			mm	0.77	
Accepted height of transducer	mm:	0.8			
Required acoustic power					
Modulation depth			n(10%)	0.1	
Relative acoustic quality			quartz -1.56	4.2	
Required acoustic power (eff.: 10 %)	W:	0.3131			
Distance between electrodes	mm:	1.8			
Q checking:	Q = 3.70778				
Bandwidth:	ΔF (MHz) 84				

Calculations were carried out for LiNbO_3 transducer (Y 36° cutting – longitudinal wave).

Table 3. Construction data and experimental errors of the phase measurements for four modulators.

Parameters	Model 0	Optimised models		
		1	2	3
Material of buffer	BK 7	SF 4	BK 7	BK 7
Transducer	LiNbO_3 (Y 36°)			
Central frequency (MHz)	140			
Dimensions of electrode (length × height) (mm)	10×1	6.8×0.8*		
Distance between electrodes** (mm)	3	1.8		
Theoretical coefficient	6	4.5		
Measurement coefficient	3.78	2.95	3.15	3.65
Amplitude of correction function (°)	15.5	1.4	5.3	9.74
Error of phase measurement (°)	3	<0,5	<0,5	2

* value calculated theoretically, precision of electrodes performance was not high.

** measured between electrodes centres.

manufactured at the Department of Acousto-optic Modulators in Institute of Optoelectronics. LiNbO₃ crystal plates attached to SF4 and BK7 glass buffers were used as piezoelectric transducers.

Compared to preliminary model, optimised modulators are characterised by considerably lower level of cross-talk energy and significant increase in phase resolution. In two cases experimental errors in phase measurements at frequency 140 MHz were lower than 0.5°.

6. Conclusions

Presented method for calculation of two-channel acousto-optic deflectors completes existing literature devoted to acousto-optic deflectors. A two-channel modulator is a key element in any acousto-optical receiver used in spectrum analysers. The paper shows construction of a device for spectrum and signal phase measurements at frequency bandwidth of 80 MHz with resolution of 0.2 MHz. Such device can be based on a cheap acousto-optic deflector made of SF4 glass.

Research on modulators performed in Institute of Optoelectronics confirms high accuracy of the phase measurement of radio-signals. Those modulators can be used for analysis and recognition of signals in mobile phones networks (digital GSM, analogue NMT) or UHF band.

References

1. W.I. Balakszij, W.N. Parygin, and L.E. Czirkow, *Fiziticheskiye Osnovy Akustooptiki*, Radio i Swiaz, Moscow, 1985. (in Russian).
2. A. Sliwinski, *Ultrasounds and their Applications*, WNT, Warsaw, 1993. (in Polish)
3. W. Ciurapiński and M. Szustakowski: "Acousto-optic RF analyser", *Proc. Acousto-electronics 87 Varna*, May 5-8, 359–362 (1997). (in Russian).
4. Annual Project Review Report COP 959, "Development of mobile communication systems on solid state elementary basis", in *Technical Audit*, Part A, 12, 1998.
5. L. Jodłowski, "Investigation of acousto-optic modulator with 500 MHz bandwidth", 1999. (unpublished)
6. L. Jodłowski, "Increase in accuracy of phase difference measurement in an acousto-optic processor due to cross-talk correction", *J. Opt. A: Pure Appl. Opt.* **3**, 77–81 (2001).
7. M. Szustakowski and L. Jodłowski, "Construction and properties of the multielement filters for matching piezoelectric transducer", *Proc. 6th Spring School on Acousto-Optics*, Jurata, 1995.
8. V. Petrov, "What about more than 2 GHz acousto-optical interaction bandwidth", *Proc. SPIE* **2969**, 217–222 (1996).
9. L. Jodłowski, "Investigation of acceptable power for piezoelectric crystal transducer", 1999. (unpublished)
10. W. Soluch, "Introduction to piezoelectronics", WKiŁ, Warszawa, 1980. (in Polish).
11. L. Jodłowski and J. Zieniuk, "Technological optimisation of LiNbO₃ mono-crystal 1 GHz transducer for ultrasonic microscopy", *Acoustic* **79**, 97–101 (1993).
12. L. Jodłowski, "Wide-band matching in acoustic heads", *Proc. 2nd Polish Conf. on Non-destructive Investigations*, Gliwice (1997). (in Polish).
13. H. Eschler and F. Weidinger, "Acousto-optic properties of dense flint glasses", *J. Appl. Phys.* **46**, 65–70 (1975).
14. A. Hilderbrandt, H. Sołtysik, and A. Zieliński, *Theory of Circuits – Exercises*, WNT, Warszawa, 1974. (in Polish).
15. J.C. Poncot, "Advanced multi channels Bragg cells for 2D interferometric phase-frequency measurements", *Int. Conf. on Optical Information Processing*, St. Petersburg, 101–109 (1993).
16. M. Buda, K. Goździk, and L. Jodłowski, "Technology and properties of connections in acousto-optic modulators" in *Works of ITR*, Part I, **100** (1985), Part II and III, **102** (1986). (in Polish)
17. M. Szustakowski, L. Jodłowski, I. Merta, and R. Bobrowicz, "An acousto-optic processor for phase and frequency measurement", *Proc. SPIE* **3581**, 196–199 (1998).

EMIS Datareviews Series

Electronic Materials Information Service and related publications

Series Advisor: Professor B.L Weiss-University of Surrey, UK

EMIS DATAREVIEWS SERIES

This series comprises books on semiconductors and other electronic materials. These adopt a unique editorial approach based wholly on commissioned input from experts around the world into a structured framework. Each book comprises numerous invited Datareviews (i.e. modules of knowledge) and combines latest specialised understanding, highly structured presentation, numeric data, individual Datareview cut-off dates, background and contextual information, expert guidance to the literature, wide but deep coverage and comprehensive subject indexing. All EMIS books are casebound, 280 x 210 mm.

Properties, growth and applications of diamond

M.H. Nazare and A.J. Neves (Eds.)

Recent breakthroughs in the synthesis of diamond have led to increased availability at lower cost. This has spurred R&D into its characterisation and application in machine tools, optical coatings, X-ray windows and light-emitting optoelectronic devices. In the longer term, diamond's high thermal conductivity and electron mobility make it potentially useful for integrated circuit applications (e.g. in heat sinks). This book draws together expertise from some 60 researchers in Europe and the USA working on bulk and thin film diamond. All fully-refereed, the contributions are combined to form a highly structured volume with reviews, evaluations, tables and illustrative material, together with expert guidance to the literature.

EM 026, 550 pages,
ISBN 0 85296 7853, 2001

£135

Properties, processing and applications of indium phosphide

T.P. Pearsall (Ed.)

In 1991, in response to strong demand by semiconductor researchers, the IEE published 'Properties of Indium Phosphide'. Since then InP has continued to be the subject of intensive R&D, especially in the area of optoelectronics, with over 11,000 papers published in the intervening period. Professor Pearsall has assembled a team of some 20 researchers from around the world in order to identify the significant advances and distil the current knowledge from this large mass of literature. New text, tables and illustrations, which form the bulk of the book, are presented together with some compressed material from the old volume.

EM 021, 300 pages,
ISBN 0 85296 949 X, 2000

£95

Physical properties of liquid crystals: Nematics

D.A. Dunmur, A. Fukuda and G.R. Luckhurst (Eds.)

The demand for liquid crystals with better display parameters and lower power consumption has stimulated much research into their properties and characterisation. A large team of some 60 leading researchers from the USA, Europe and Japan have focused their expertise to extract and review data on a wide range of properties of nematics, including those which are essential to the development of all types of liquid crystal device. Where appropriate these properties are also explained with expert commentary. The book is fully illustrated and structured for reference.

EM 025, 696 pages,
ISBN 0 85296 7845, 2000

£165

Properties of crystalline silicon

R. Hull (Ed.)

Silicon, as used in silicon chips, is the material on which the information society depends for its power to process information. In 1988 INSPEC published the standard reference source on silicon properties and since then an enormous amount of Si R&D has taken place, with a hundred thousand papers published over 1989-1998. Now, for the benefit of academics, process developers and device simulation engineers working in the area of silicon microelectronics Professor Hull has brought together the specialised expertise of over 100 invited authors from the USA, Japan and Europe coordinated by 18 chapter editors to concisely review its properties in a structured way.

EM 020, 1042 pages,
ISBN 0 85296 933 3, 1999

£195

Properties, processing and applications of glass and rare earth-doped glasses for optical fibres

D.W. Hewak (Ed.)

RETD on optical fibres is driven by the need for ever higher bandwidth transmission in telecommunications at lower cost. Some 60 experts from leading R&D groups around the world review silica, oxide, halide and chalcogenide glasses in a structured format, thereby creating an authoritative, encyclopaedic reference source for researchers and engineers. The book includes a historical overview by W. Alexander Gambling, FRS. Over 60 individually-authored modules on the above-mentioned types of glass covering optical, thermal and mechanical properties, RE spectroscopy, optical fibre manufacture and applications in fibre amplifiers, fibre gratings, fibre lasers and optical switches.

EM 022, 395 pages,
SBN 0 85296 952 X, 1998

£125

Properties of amorphous silicon and its alloys

T.M. Searle (Ed.)

Over the last decade there have been major advances in the characterisation of amorphous silicon for use in solar cells, TFT liquid crystal displays, photodetectors, LEDs and xerographic devices. In the last decade, researchers have succeeded in dispelling much of the uncertainty about its behaviour and the associated models, so that engineers are better able to exploit it. Here the essential knowledge of the properties, preparation and exploitation of amorphous silicon are distilled into one volume.

EM 019, 440 pages
ISBN 0 85296 922 8, 1998

£135

<http://www.iee.org.uk/publish/books/emis.html>